JACS
JOURNAL OF THE AMERICAN CHEMICAL SOCIETY

Article

pubs.acs.org/JACS

Reactivity Models of Hydrogen Activation by Frustrated Lewis Pairs: Synergistic Electron Transfers or Polarization by Electric Field?

Tibor András Rokob,[†,‡] Imre Bakó,[‡] András Stirling,[‡] Andrea Hamza,[‡] and Imre Pápai*[,‡]

[†]Institute of Organic Chemistry and Biochemistry, Academy of Sciences of the Czech Republic, Flemingovo nám. 2, 16610 Prague 6, Czech Republic

[‡]Institute of Organic Chemistry, Research Centre for Natural Sciences, Hungarian Academy of Sciences, H-1025 Budapest, Pusztaszeri út 59-67, Hungary

Supporting Information

ABSTRACT: Two alternative qualitative reactivity models have recently been proposed to interpret the facile heterolytic cleavage of H_2 by frustrated Lewis pairs (FLPs). Both models assume that the reaction takes place via reactive intermediates with preorganized acid/base partners; however, they differ in the mode of action of the active centers. In the electron transfer (ET) model, the hydrogen activation is associated with synergistic electron donation processes with the simultaneous involvement of active centers and the bridging hydrogen, showing similarity to transition-metal-based and other H_2-activating systems. In contrast, the electric field (EF) model suggests that the heterolytic bond cleavage occurs as a result of polarization by the strong EF present in the cavity of the reactive intermediates. To assess the applicability of the two conceptually different mechanistic views, we examined the structural and electronic rearrangements as well as the EFs along the H_2 splitting pathways for a representative set of reactions. The analysis reveals that electron donations developing already in the initial phase are general characteristics of all studied reactions, and the related ET model provides qualitative interpretation for the main features of the reaction pathways. On the other hand, several arguments have emerged that cast doubt on the relevance of EF effects as a conceptual basis in FLP-mediated hydrogen activation.

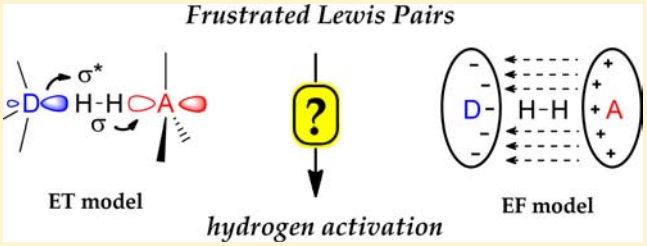

INTRODUCTION

Molecular hydrogen has significant actual and potential applications as a clean source of energy and as an atom-efficient reactant in organic synthesis. However, H_2 has low reactivity due to its fairly strong, apolar covalent bond and low polarizability. Only a limited range of chemical systems can activate it directly under mild conditions and thus act as catalysts in H_2-based processes of interest. Understanding the similarities and differences among such systems may contribute to the development of more efficient or alternative approaches.

The majority of Nature's and man-made H_2-activating systems contain transition metal atoms. In metal−ligand complexes, depending on the particular metal and the ligand set, several pathways for the reaction with H_2 have been characterized.[1−4] One possibility is splitting of H_2 via oxidative addition to yield metal dihydride compounds, often encountered with Rh- and Ir-based homogeneous hydrogenation catalysts.[1,5] The reaction can be explained by two cooperative electron transfer (ET) processes: a donation from the σ orbital of H_2 to a suitable empty d orbital on the metal, and a back-donation from a filled d orbital of appropriate symmetry to $\sigma^*(H_2)$ (Figure 1a). Both interactions lead to weakening of the H−H bond, and eventually, two M−H bonds can form. No free radicals are involved in the process, yet the shape of the orbitals leads to negligible or zero polarization of the H−H bond. This cleavage is therefore termed as *homolytic*.[6] As an alternative, a ligand may assist in the cleavage process by removing a proton from a metal−H_2 complex, as typical for Ru catalysts and the hydrogenase enzymes.[1,5,7] This kind of *metal-based heterolytic* hydrogen cleavage can also be rationalized as the result of cooperative ETs, with $\sigma(H_2)$ donating to a metal d orbital and $\sigma^*(H_2)$ accepting from some filled orbital (often the lone pair) of the Lewis donor (Figure 1b).[8]

Besides the most prevalent transition metal compounds, an increasing number of main-group systems have been reported to promote easily the cleavage of the H−H bond. In 2007, Schoeller, Bertrand, and co-workers reported facile addition of H_2 to singlet (alkyl)(amino)carbenes at room temperature and atmospheric pressure.[9] Their detailed mechanistic analysis revealed that the carbene lone pair and the empty carbon p orbital can act similarly to metal d orbitals (Figure 1c) and provide simultaneous electron donation from and back-donation to H_2. Interestingly, the back-donation to $\sigma^*(H_2)$ cannot occur symmetrically, and the H_2 molecule is polarized during its conversion to the product containing two identical C−H bonds. This reactivity is not limited to low-valent carbon compounds since related (amido)(boryl)silylenes,[10] diaryl

Received: December 19, 2012
Published: February 23, 2013

   dx.doi.org/10.1021/ja312387q | J. Am. Chem. Soc. 2013, 135, 4425−4437

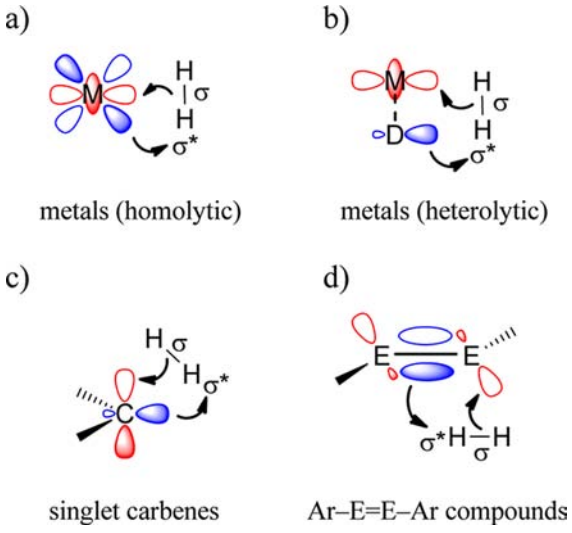

Figure 1. Various modes of hydrogen activation: (a) metal-based homolytic, (b) metal-based heterolytic, (c) singlet carbene, and (d) Ar−E═E−Ar compounds with E = Ge, Sn. Occupied donor orbitals are shown in blue, unoccupied acceptor orbitals in red.

germylenes,[11] and diaryl stannylenes[12] also undergo similar reactions with H_2. The doubly bound, bent relatives of acetylene, Ar−Ge═Ge−Ar[13] and Ar−Sn═Sn−Ar,[14] provide a further possibility for hydrogen activation. Mechanistic studies uncovered that, in the initial step, electrons are donated from H_2 to an empty nonbonding orbital, formed from sp^2-like orbitals on the Ge/Sn atoms, while back-donation is also operative from the π bonding orbital of the double bond (Figure 1d).[15]

In the mid-2000s, a new chapter was opened in transition-metal-free hydrogen activation by the experiments of Stephan's research group. The covalently linked, sterically demanding phosphinoboranes $R_2P-C_6F_4-B(C_6F_5)_2$ (R = ^{t}Bu, Mes) were shown to activate H_2 easily, resulting in zwitterionic phosphonium borates $[^+HR_2P-C_6F_4-B(C_6F_5)_2H^-]$.[16] Later, simple combinations of bulky phosphines and boranes (R_3P/$B(C_6F_5)_3$, R = ^{t}Bu, Mes) were also demonstrated to exhibit similar reactivity and yield $[R_3PH]^+[HB(C_6F_5)_3]^-$ salts at 25 °C and 1 atm of H_2 pressure.[17] In the recent years, there has been a spectacular development in this field, and a wide variety of P, N, C, O donors and B, Al, Si acceptors have been reported to be active toward H_2 in intra- or intermolecular combinations and also to act as hydrogenation catalysts.[18−20] These bulky Lewis pairs have been termed[21] "frustrated Lewis pairs" (FLPs) on the basis of their tendency not to form classical donor−acceptor dative bonds. Besides H_2, they also react with a series of other small molecules or bonds.[18]

In the hydrogen activation reaction by the prototypical ^{t}Bu$_3$P/B$(C_6F_5)_3$ pair, no intermediate was observed experimentally.[17] We therefore initiated a computational study in 2007 to gain detailed atomistic insight.[22] We identified a single, early transition state (TS) along the reaction pathway from the reactants to the products, in which the H_2 is close to the P and B centers and interacts with them simultaneously. From our results, we proposed a general reactivity model corresponding to the same principle as all reactions discussed above. Namely, synergistic ETs, in this case from the lone pair of the Lewis base to $\sigma^*(H_2)$ and from $\sigma(H_2)$ to the empty orbital on the Lewis acid, lead to weakening and, ultimately, to heterolytic cleavage of the H−H bond (see Figure 2a). The absence or easy dissociation of the dative adduct between the Lewis

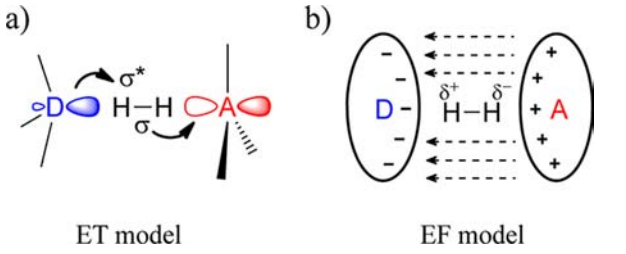

Figure 2. (a) Electron-transfer-based and (b) electric-field-based models for hydrogen cleavage by frustrated Lewis pairs.

components was pointed out to provide a reactant state destabilization that lowers the barrier and increases exothermicity. As a further key ingredient relevant for unlinked FLP systems, we highlighted that the noncovalent interactions between the bulky substituents can lead to the formation of weak, flexible adducts of the Lewis pair where the donor and acceptor centers are intact and preorganized for the reaction with the incoming H_2 molecule. These adducts were termed as "frustrated complexes" or "encounter complexes", and our later computations[23] involving explicit solvent confirmed that they can be present in small but relevant concentration in solution. From a detailed study on the electronic structure of the involved species,[24] we furthermore concluded that the barrier mostly originates from the energetic cost of creating the orbital overlaps and distorting the individual donor and acceptor molecules. The distortion of the frustrated complex was found to provide only a minor contribution to the activation energy. For intramolecular FLPs with appropriate linkers, the necessary preorganization of the active centers may be provided by the covalent backbone at a significantly lower entropic cost.

Later, Grimme and co-workers reinvestigated the ^{t}Bu$_3$P/B$(C_6F_5)_3$ + H_2 reaction, and they outlined a conceptually different mechanistic scenario.[25] The new proposal is based on the statement that the frustrated complex possesses significant electric field (EF) in its interior (Figure 2b). High-level computations showed that H_2 exposed to sufficiently strong homogeneous EFs can be cleaved heterolytically in a barrierless process, and the authors indeed found that H_2 forced into a geometry with linear alignment of the reacting PHHB four-atom fragment inside the FLP undergoes barrierless cleavage. According to their interpretation, there is thus no need to consider specific FLP/H_2 orbitals or electron donation processes to understand the essence of the activation process. They described the TS of the process as corresponding to the "entrance" of H_2 into the cavity of the FLP, thereby corresponding to a "preparation" step, which allows H_2 to reach the region with high EF strength. In that region, heterolytic cleavage without barrier can occur. The similar chemical behavior of various FLPs was suggested to originate from the similar EFs they generate. Although the incompleteness of this simple, FLP-free approach was clearly stated,[25] and the model was emphasized to be "*appropriate only for the initial part of the reaction*",[26] it was still concluded to correspond to a new mechanistic scenario, helping to design new FLP chemistry, and not to an extension of the previous proposal.[25]

Since its publication, this alternative picture has been widely regarded[2,18a,19e,20l,u,27] as the modern view of FLP-type reactivity, yet its perhaps most thought-provoking aspect has

dx.doi.org/10.1021/ja312387q | J. Am. Chem. Soc. 2013, 135, 4425−4437

Chart 1. Investigated Frustrated Lewis Pairs

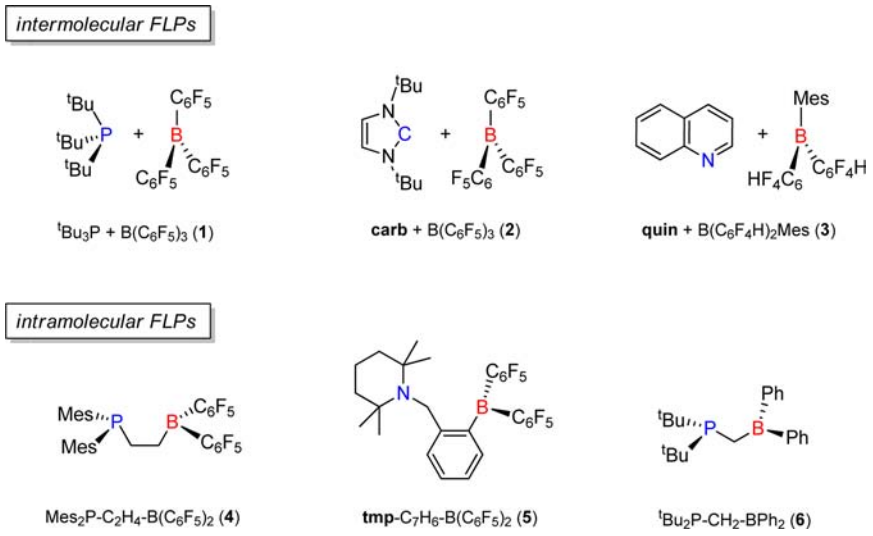

seldom been recognized. Namely, it points to a mechanistic divergence from other nonradical H_2 cleaving systems shown in Figure 1, immediately raising a series of questions. Do the FLPs thereby occupy a unique position, with a chemistry formally similar but in its grounds distinct from what was known before? Or should other heterolytic cleavages be reconsidered as well, and the EF model has a wider applicability? Can it be applied, for example, to the "borderline-case" heterolytic cleavage by carbenes, where the hydrogen atoms end up in equivalent, relatively apolar bonds? It seems that intriguing answers could be obtained from detailed comparisons of the two conceptual models, and the obtained clearer insight could be expedient for both theoretical and synthetic chemistry.

To our knowledge, only one study has appeared in the literature with the aim of assessing the relevance of orbital and EF effects. In this work of Camaioni et al.,[28] reactions of simple Lewis pairs (NH_3 + BX_3, X = H, F, Cl) with H_2 were investigated, and detailed analysis of the electronic structure and interaction energies was given. The authors found that structural reorganization of the precursor complex plays a significant role in dihydrogen activation, and charge-transfer interactions are the dominant stabilizing factors in the TS. It was concluded that the EF created by the NH_3/BX_3 pair has a polarizing effect, but its contribution to the overall interaction energy is small compared to that from orbital overlaps, thus the EF alone is not sufficient to cleave the H_2 molecule. Whether the EF generated by real FLPs is stronger or more effective in this respect is an immediately relevant question.

However, though electrostatic polarization and orbital overlaps are obviously two ingredients of molecular interactions, the original mechanistic studies suggested either the ET alone[22] or the polarization by EF alone[25] to provide foundation for stand-alone reactivity models that can account for the essence of H_2 cleavage and thus serve as a guiding principle in designing new systems. It would be therefore of even greater interest to compare the predictive power of the two incommensurable models in the qualitative interpretation of the features of the H_2 cleavage reaction.

In our present computational contribution, we thus aim to assess the ability of the two incompatible reactivity models to explain H_2 cleavage by FLPs. Unlike in the previous works,[22,25] we treat a wider, representative set consisting of six FLPs, all of which have been characterized experimentally. For the observed H_2 activation reactions, we locate the corresponding TSs and characterize their electronic structure and the EF generated by the FLP. Furthermore, results about structural and electronic rearrangements and the EFs along the corresponding reaction pathways are analyzed. The computed characteristic features are compared with qualitative predictions from the two models, and the merits and limitations of the two contrasting mechanistic descriptions are discussed. From the analysis, it seems clear that the EF-based interpretation of H_2 cleavage can be seriously questioned.

COMPUTATIONAL DETAILS

Throughout this study, density functional theory (DFT) with the dispersion-corrected, range-separated hybrid ωB97X-D exchange-correlation functional[29] was employed. For geometry optimization, vibrational frequency determination, electronic structure analysis, and calculation of EFs, we employed the 6-311G(d,p) polarized triple-ζ basis set.[30] Single-point energies were calculated with the larger, 6-311++G(3df,3pd) basis.[30] We carried out a series of test calculations on the $^tBu_3P/B(C_6F_5)_3$ pair to assess the dependence of the results on the level of theory. These tests, presented in the Supporting Information (SI, section S.1), demonstrate that several different functionals performing well[31−34] for dispersion interactions and reaction barriers, namely ωB97X-D, M06-2X[35] and PW6B95-D3,[36,37] yield very similar data. Close agreement was furthermore obtained using the less satisfactory but often applied B3LYP-D3[37,38] functional, and the nature of the electronic rearrangements can be correctly identified even in the TS located without dispersion corrections. Changing the basis set used in the analysis to 6-31G(d) or 6-311++G(3df,3pd) does not alter significantly the numerical values either. In short, our conclusions are independent of the specific method chosen.

For all considered reactions, the located minima and TSs possess the expected zero and one imaginary vibrational frequency, respectively. Starting in both directions from the TSs, we determined the minimum energy pathway in mass-weighted Cartesian coordinates, i.e., the intrinsic reaction coordinate (IRC) path, using a Hessian-based predictor-corrector algorithm.[39] As we are now interested in the inherent electronic properties of the reactions rather than in reproducing experimental reaction rates, we present electronic energy data without zero-point or solvent corrections. All geometry optimizations and frequency calculations were done with Gaussian 09,[40] except for the PW6B95-D3 and B3LYP-D3 tests, for which Turbomole 6.3[41] was employed. Electric field vectors and their

dx.doi.org/10.1021/ja312387q | J. Am. Chem. Soc. 2013, 135, 4425−4437

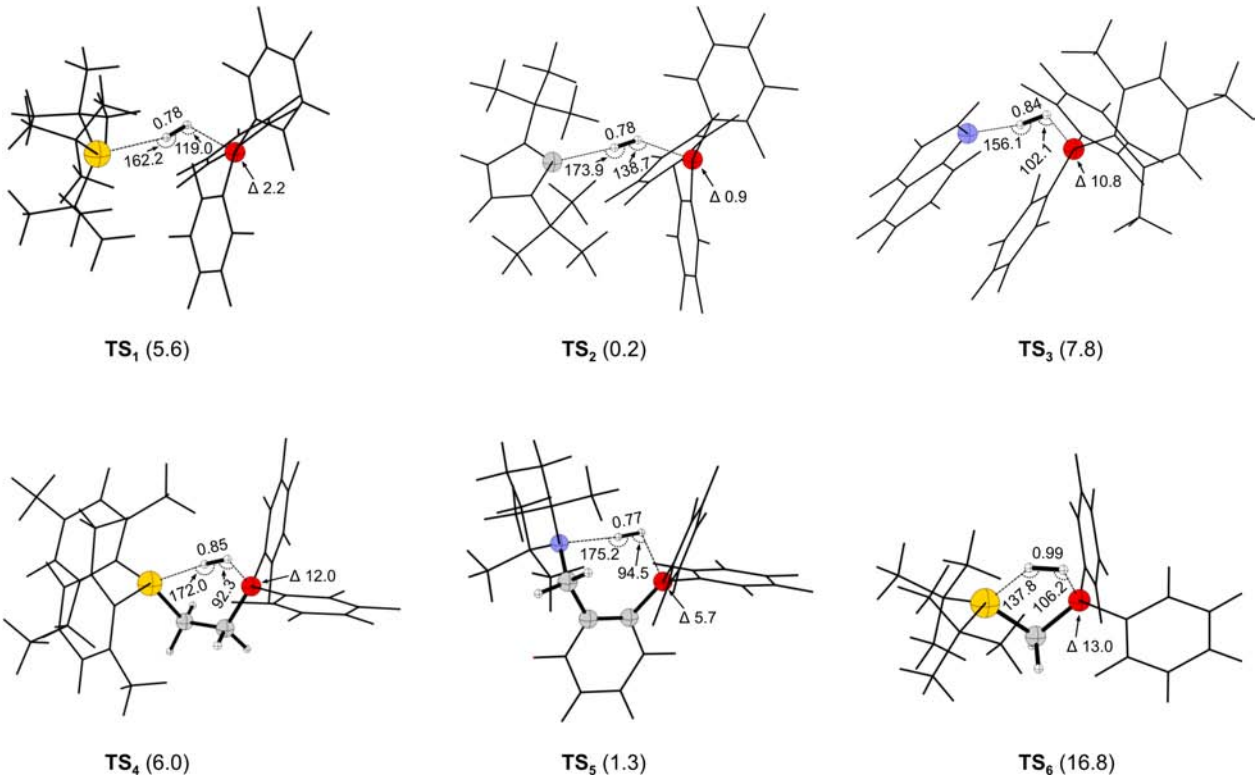

Figure 3. Transition states for H_2 cleavage by the six FLPs, optimized at the ωB97X-D/6-311G(d,p) level. Reported geometrical parameters are H−H distances (Å), donor atom−H−H and H−H−acceptor atom angles (degrees), and the deviation of the sum of the C−B−C angles around the boron from 360° (denoted by Δ, in degrees). For each TS, relative electronic energy with reference to free H_2 plus the frustrated complex (**1**−**3**) or to free H_2 plus the datively unbound, prepared conformer (**4**−**6**) is given (in kcal/mol). Free H_2 has a bond length of 0.74 Å at the applied level of theory. The deviation Δ would be 0° for a planar and 31.6° for a completely pyramidalized, ideal tetrahedral center.

magnitudes were computed using our own routines carrying out finite-difference derivation of the molecular electrostatic potential. To this end, the potential was first calculated by Gaussian's *cubegen* on a grid containing the desired points; then, the calculation was repeated on three more grids shifted in *x*,*y*, and *z* directions by a step size of 0.005 Å, which was checked to yield results of sufficient accuracy for the present purposes. Natural Population Analysis and Natural Bond Orbital analyses[42] were carried out with the NBO 3.1 program as included in Gaussian, and Mayer bond orders[43] were determined using the BO-SPIN program.[44] Molecular structures were plotted using XYZViewer.[45]

RESULTS

Investigated Frustrated Lewis Pair Systems. In order to explore the performance of the two reactivity models in the interpretation of a wider range of reactions, we included six FLPs in our study (Chart 1). The list contains simple donor/acceptor pairs (**1**−**3**) and covalently linked compounds (**4**−**6**) with phosphorus (**1**, **4**, **6**), nitrogen (**3**, **5**), and carbon (**2**) donor atoms. On the acceptor side, only boron compounds are treated, which reflects that boron has almost exclusively been used as the acceptor atom of FLPs. Nevertheless, besides the most extensively utilized tris(pentafluorophenyl)borane $B(C_6F_5)_3$ (**1**, **2**) and bis(pentafluorophenyl)boryl group (**4**, **5**), we also examined boranes with increased steric demands (**3**) and notably decreased acidity (**6**).

Each system has been the subject of both experimental and computational studies previously. The absence of dative bond and the facile H_2 cleavage with the $^tBu_3P/B(C_6F_5)_3$ pair (**1**) were observed by Stephan et al.,[17] and this system has been treated as a paradigm case of FLPs by many theoretical contributions since then.[22−25,46−50] Activity of the carbene/borane pair **2** was independently discovered by Stephan's[51] and Tamm's[52] groups. While showing no carbene−borane interaction at −78 °C, this system slowly loses its activity at room temperature due to a side reaction. Tamm and co-workers also provided a computational interpretation of the observed H_2 cleavage and self-deactivation reactivities.[52] For the quinoline/borane system **3**,[20f] equilibrium between the datively bound and free forms was found at room temperature. The primary product of the H_2 cleavage, i.e., $[\mathbf{quin}H]^+[HB(C_6F_4H)_2Mes]^-$, has not been observed directly because the reaction proceeds further to give partially reduced quinoline derivatives, but its existence was inferred from detailed experimental and computational mechanistic investigations. The alkylene-linked phosphine−borane system **4** was described by Erker et al.,[53] who found that a P−B bond is present and suggested the open form to be responsible for H_2 activation. This suggestion was computationally confirmed in Grimme and co-workers' study.[25] The nitrogen/boron "molecular tweezer" **5**, reported and theoretically analyzed by Repo and Rieger et al.,[20v,54] is the only compound in our series for which H_2 loss upon heating the product was detected, i.e., the H_2 activation is reversible. No N−B dative bond was observed in this case. Finally, the "preorganized" FLP of Slootweg, Lammertsma et al. (**6**)[20b] represents a rare example of FLPs that are active toward H_2 but contain no fluorine atoms. Lewis donor−acceptor bond is also absent for this compound.

With one exception, all examined pairs yield the isolable ionic or zwitterionic H_2 cleavage products within minutes or hours at room temperature and 1 atm of H_2 pressure. For the quinoline/

Table 1. Electronic Structure Parameters of the Transition States[a]

		Mayer bond orders			atomic charges[b]			
FLP	H−H distance (Å)	donor−H	H−H	H−acceptor	H_D	H_A	donor	acceptor
1	0.78	0.09	0.77	0.20	0.15	−0.07	0.11	−0.19
2	0.78	0.18	0.80	0.16	0.14	−0.12	0.09	−0.11
3	0.84	0.20	0.51	0.43	0.35	−0.02	0.12	−0.45
4	0.85	0.21	0.52	0.40	0.23	0.03	−0.26	
5	0.77	0.13	0.75	0.21	0.16	−0.01	−0.15	
6	0.99	0.45	0.39	0.53	0.16	−0.07	−0.09	

[a]All calculations at the ωB97X-D/6-311G(d,p) level of theory. The H−H distance is provided as a measure of the early nature of the TS (cf. the 0.74 Å equilibrium distance). The Mayer bond order of free H_2 is 1.00 as expected. [b]From Natural Population Analysis. H_A/H_D = the hydrogen atom closer to the acceptor/donor center; "acceptor"/"donor" = atomic charges summed for all atoms of the acceptor/donor molecule, or for the whole linked FLP.

borane system **3**, more forcing conditions were necessary (105 °C, 4 atm), and during this reaction, only the neutral, 1,2,3,4-hydrogenated quinoline was observed in the solution besides the starting materials.[20f]

The Nature of Transition States. The starting point of our computational analysis of the six H_2 cleavage reactions is a comparison of the general features of the TSs, including the question whether the incoming H_2 has undergone any notable activation. The geometries of all TSs considered here have been published at various levels of theory;[20b,f,v,22,24,25,50,52,54−56] now, we present a comparison on the basis of ωB97X-D/6-311G(d,p) results (Figure 3).

Apparently, H_2 interacts with both active centers in each case since the donor−H and H−acceptor distances are notably smaller than the corresponding sums of the van der Waals radii.[57] The H−H bond is always elongated with respect to the free H_2 molecule, and the extent of this elongation varies along the series. Namely, $\mathbf{TS_1}$, $\mathbf{TS_2}$ and $\mathbf{TS_5}$ represent rather early TSs with a H−H distance at most 0.04 Å larger than the equilibrium bond distance, but in $\mathbf{TS_3}$, $\mathbf{TS_4}$, and particularly in $\mathbf{TS_6}$, the stretching can reach 0.1−0.2 Å. The deviation of the sum of the C−B−C angles around the boron from 360° (denoted by Δ in Figure 3) points to incipient pyramidalization of the borane, which occurs in correlation with the elongation of the H−H bond. Accordingly, for $\mathbf{TS_1}$, $\mathbf{TS_2}$, and $\mathbf{TS_5}$, the deviation amounts only to 1−6°, but for $\mathbf{TS_3}$, $\mathbf{TS_4}$, $\mathbf{TS_6}$, it somewhat exceeds 10°. Considering that an ideal tetrahedral center has a Δ value of 31.6°, these structures are ∼30% pyramidalized.

A further notable feature of the TS geometries is the shape of the four-atom fragment consisting of the cleaved H_2 and the interacting donor and acceptor atoms, hereafter referred to as the DHHA unit. Although the DHH angle is consistently ∼160−180° (with the exception of $\mathbf{TS_6}$, 137.8°), the HHA angle is *always* smaller, typically falling into the 90−120° range. The DHHA fragment thus has a characteristic bent arrangement, with a general tendency for end-on D···H_2 and side-on H_2···A interactions, somewhat similarly to a μ-(η^1,η^2) coordination. A slight or marked deviation from linearity is present in all FLP H_2 activation TS geometries described in the literature, but this property has been highlighted only in a couple of works.[20o,25,28,52,58−60] As pointed out by Grimme and co-workers,[25] theoretical methods performing poorly for dispersion interactions tend to overestimate the D···A distance, and consequently, underestimate the bending. This inaccuracy is admittedly present in the B3LYP TS geometry reported in our earlier work[22] as well; nevertheless, the preference for end-on D···H_2 and side-on H_2···A arrangement is still recognizable even at that level of theory.[61] Accordingly, a linear or almost linear TS was not considered as an integral part of the ET model, nor was it stated that such geometry would arise from its basic assumptions.

Further information about the extent of activation in the TSs can be obtained by characterizing the pertinent electronic rearrangements, for example, using the atomic charges and bond orders associated with the involved atoms. Although unambiguous definitions for these quantities do not exist, important insights can still be obtained from their examination.[62] For the TSs of the present reactions, they are collected in Table 1. The most striking observation is that the H−H bond orders are as low as 0.7−0.8 even for the earliest TSs, pointing to a significantly activated H_2. In later TSs, the bond may be more than half-way to being broken, with bond orders of 0.4−0.5. The weakening of the H−H bond is accompanied by the formation of partial acceptor−H and H−donor bonds, the acceptor−H typically being in a more advanced stage.[63] Along with the emerging bond breakage, notable polarization of H_2 is also a general phenomenon, as apparent from the different atomic charges on the two H atoms. The difference is on the order of ∼0.2 elementary charge, with no apparent dependence on the lateness of the TS. Importantly, the direction of the polarization always corresponds to the eventual bond cleavage; i.e., the hydrogen close to the donor center becomes positive. Furthermore, all intermolecular FLPs show a net ET from the donor to the acceptor molecule. The present results thus indicate that significant electron reorganizations taking place already at the TS with the involvement of donor/acceptor partners and the bridging H_2 molecule are common features of all studied H_2 splitting reactions. The computed electronic properties are in line with those of our early B3LYP study on **1**,[22] implying that the nature of the TS and the underlying chemistry were correctly identified at that time, in spite of the inaccurate geometry.[64]

Concerning the energetics of the TS, we found that the hydrogen activation itself does not have high energy demands in any of the considered reactions. The computed electronic barriers are shown in Figure 3. For the intermolecular FLPs, they were calculated with respect to the energy level of isolated H_2 plus the frustrated complex, while for the intramolecular FLPs, they are referenced to isolated H_2 plus the "prepared" FLP conformer, i.e., the local minimum structure containing no dative bond. The highly exothermic carbene−borane system **2** has a barrier of a mere 0.2 kcal/mol, and for the intramolecular amine−borane system **5**, we also calculated a small activation energy of only 1.3 kcal/mol. The other limit, 16.8 kcal/mol, is set by FLP **6** with reduced acidity. The remaining FLPs require 5−8 kcal/mol activation energy. Note that these values do not

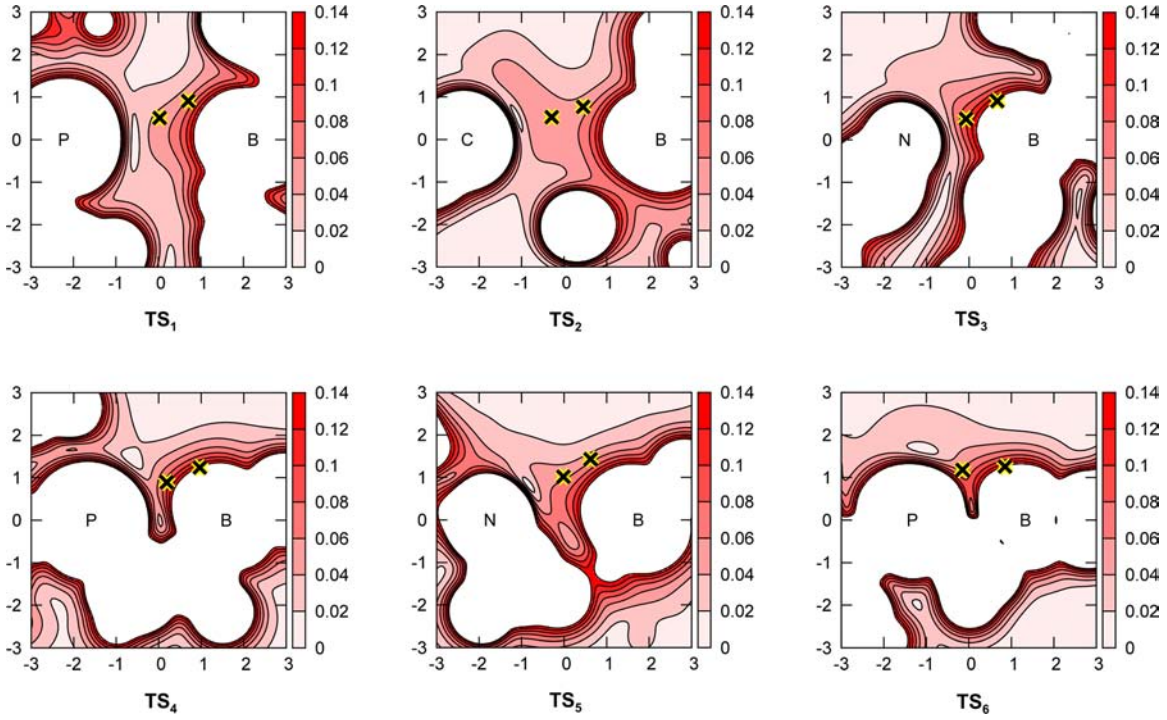

Figure 4. Magnitude of the electric field generated by FLPs **1**–**6** in their TS geometry. The atoms of the cleaved H_2 were not included in the calculation; only their positions are recorded and shown as yellow/black crosses. The field strength is computed in the points of a 6 × 6 Å^2 plane, defined by the two H atoms and the midpoint of the donor–acceptor axis. As the donor and acceptor atoms lie very close to this plane, their projected position is also marked with the corresponding atomic symbols. Distances along the plane edges are given in Å, EF strength in atomic units. Areas where the field strength exceeds 0.14 au (e.g., close to the donor and acceptor or other nuclei) are left white.

correlate directly with the observed reactivities as we intentionally do not take into account here solvent effects, the energy required to break the dative bond in **4**, and the different activation entropies of the linked and intermolecular systems.

Interpreting Transition State Properties. The characteristics of computationally located TSs, particularly of those that are rate- or turnover-determining, bear utmost importance in the understanding of chemical reactions. The geometric and electronic structure of the calculated TSs usually reflect the most important interactions governing the actual chemical behavior, and one can hardly advance toward the rational design of more efficient systems without exploring these interactions. For this reason, we now examine how the calculated TS properties can be rationalized by the EF-based and ET-based reactivity models.

The reduced H–H bond order, the polarization, the charge redistribution and for some FLPs, the appreciable lengthening of the H–H distance and the pyramidalization of the borane all support a view that describing the TS in the EF model as corresponding to an "entrance" step is quite misleading. This term would suggest the passage of an essentially intact H_2 molecule into the interior of the FLP, hindered only by steric repulsion and the unfavorable deformation of the frustrated complex, which is obviously not the case. Such a process is also inconsistent with the fact that the TSs share qualitative features with respect to the mutual alignment of the approaching H_2 and the donor/acceptor centers. Nevertheless, within the framework of the EF model, we may still investigate whether the EFs generated by the FLPs provide an adequate interpretation of the TS. To do so, we first recall Grimme and co-workers' results about the effect of a homogeneous field on the H_2 molecule.[25] They found that a field strength of 0.09–0.10 au is necessary to lower the H–H splitting barrier into a reasonable range (20 kcal/mol or lower).[65] Notably, the activation energy for H_2 cleavage increases very quickly for smaller field strengths; at 0.08 and 0.06 au, it is ∼40 and ∼80 kcal/mol, and the H–H distance at the barrier is ∼1.8 and ∼2.4 Å, respectively. Concerning the actual field strength in the FLPs, very limited amount of information is available in the literature. Only a concise textual description of the field of **1** and **4**,[25] as well as an analysis about a nonfrustrated model system,[28] has been presented. In Figure 4, we therefore show two-dimensional plots of the strength of the EF generated by the frustrated pairs **1**–**6** in the TS geometry.

The most obvious property, apparent from these plots, is that the fields are extremely inhomogeneous. In contrast to the suggestion of the EF model, no region can be clearly identified as the "cavity" of the frustrated pair having a field strength appropriate for sufficiently reducing the H–H activation barrier, i.e., ∼0.09 au or larger. In TSs with relatively large D···A distances (**TS$_1$** and **TS$_2$**), the field strength in between the active centers (i.e., in the "interior" of the FLPs) is much weaker (0.02–0.04 au), whereas in more compact TSs (**TS$_3$**–**TS$_6$**), this region cannot be accessed by the H_2 molecule for steric reasons. Large EF strengths do appear in spherical domains in the vicinity of the P/N/C/B atoms, but one has to keep in mind that the H nuclei do not get closer to them than the equilibrium X–H distances in the products (1.0–1.4 Å). In TSs where H_2 approaches these spherical regions, the magnitude of the field experienced by the two H atoms may still be significant, up to ∼0.14 au (e.g., in **TS$_3$** or **TS$_4$**), while in other TSs, values of ∼0.04–0.06 au are typical (e.g., in **TS$_2$** or **TS$_5$**). Importantly, the direction of the EF vector does not

dx.doi.org/10.1021/ja312387q | J. Am. Chem. Soc. 2013, 135, 4425–4437

coincide with the H−H bond, particularly not in the spherical regions where it usually points radially outward from the P/C/N/B atoms.[66] Hence, it is more instructive to look at the field component parallel to the H−H axis as only this is relevant to the heterolytic bond cleavage. These parallel projections along the H−H axes in the TSs are compared in Figure 5.

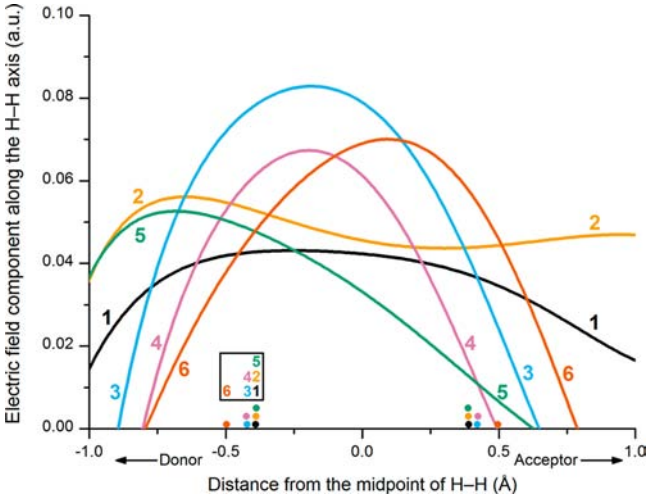

Figure 5. Electric field component parallel to the H−H direction, computed in the points along the axis of the H_2 molecule in the TS geometries of FLPs **1**−**6**. The atoms of the cleaved H_2 were not included in the calculation. The midpoint of H_2 is always at the zero of the distance scale, and the positions of the H atoms are shown by the filled circles near the *x* axis. The H atom closer to the acceptor has positive distance. Positive EF component values correspond to a field pointing from the acceptor toward the donor, i.e., in the direction facilitating the eventual cleavage.

Although the sign of the parallel component is appropriate to polarize H_2 in the observed direction and facilitate the H_2 cleavage for all FLPs, the magnitude of the parallel component remains below, often well below, ∼0.08 au, implying that up to the TS along the reaction pathway, the H_2 molecule does not reach a field strength that would explain its cleavage in terms of barrier height or H−H distance. The bond order of an H_2 molecule does decrease in EF, but the change is notably smaller than the values computed in the presence of FLP components.[67] It thus seems that the EF generated by an FLP is alone insufficient to interpret H_2 cleavage, similarly to the case of simple NH_3 + BX_3 pairs.[28]

Turning our attention to qualitative features and predictions within the EF model, it is apparent that the examined systems display very diverse fields, both in terms of strength and variation along the H−H axis. This contradicts sharply with one of the propositions of the EF model, namely that the similar chemical behavior of FLPs originates from similar field characteristics. The incipient donor−H and H−acceptor bonds and the net ET from the donor to the acceptor are far from being negligible already at this stage of the reaction, but they are admittedly not part of the EF model at all. Finally, the EF alone provides no explanation for the observed bent geometry. The polarizability of H_2 is the largest along its axis, and thus orientation of the H−H direction parallel to the EF vector would be expected. However, the angles between the H−H axis and the EF vector are computed to be ∼45° on average in the TSs,[68] which contradicts the above principle. Grimme and co-workers noted[25] that the geometry can be influenced by the polarity and the interfragment distance of the FLP, but no details were given as to what specific arrangement these effects would induce.[69,70]

In contrast to the above, the ET-based model provides a consistent interpretation of the TS features. First, we found that in the investigated six FLPs at the TS geometry, the anticipated occupied donor lone pair and empty acceptor orbitals are always present and appropriate for an interaction with H_2. These orbitals typically correspond to the highest occupied molecular orbital and lowest unoccupied molecular orbital of the FLP, respectively.[71] This result is in line with the expectations based on chemical intuition as well as with earlier calculations on various FLPs.[20b,24,50,59,72−78] Natural Bond Orbital analysis confirms that the donor/acceptor orbitals are in significant interaction with $\sigma^*(H_2)/\sigma(H_2)$.[79] The population of the $\sigma^*(H_2)$ and depletion of the $\sigma(H_2)$ orbitals explain the H−H bond order decrease. At the same time, the overlaps between the donor orbital and $\sigma^*(H_2)$ as well as between the acceptor orbital and $\sigma(H_2)$ account for the forming D−H and H−A bonds and for the appearance of charges on the components of intermolecular donor/acceptor systems (see Figure 6). These overlaps are enhanced by a mixing of the $\sigma(H_2)$ and $\sigma^*(H_2)$ orbitals, which leads to the polarization[24,80,81] of H_2 and also contributes further to bond order decrease. The proposed synergistic nature of the electron donation processes is nicely reflected by the cooperative effects found by Grimme et al. for **1** in a linear DHHA arrangement,[82] and identified by us for **1**−**3** in the TS geometries.[83] By continuously strengthening these key interactions, one can describe the whole spectrum of electronic structures from the intact reactants to the fully formed products. As expected, the TS appears at a midpoint on this spectrum, showing notable activation with respect to the reactants but not yet corresponding to the products.

Regarding the specific end-on D···H_2 and side-on H_2···A arrangement of the reacting partners, the ET model provides a very simple explanation. As illustrated in Figure 7, an idealized

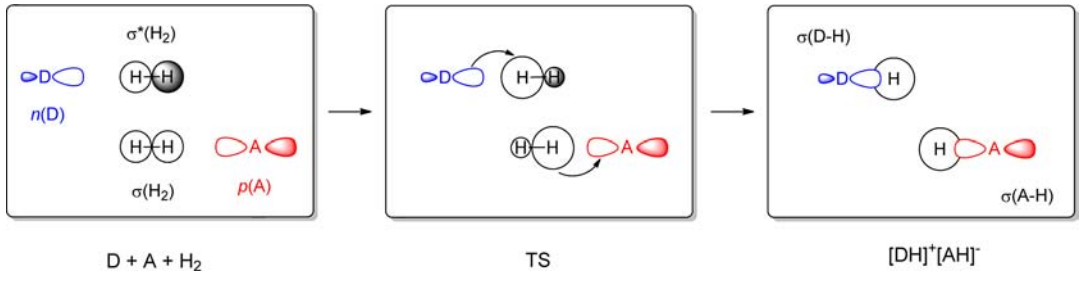

Figure 6. Electron-transfer-based interpretation of polarization and cleavage of H_2 and the formation of new D−H and H−A bonds.

dx.doi.org/10.1021/ja312387q | J. Am. Chem. Soc. 2013, 135, 4425−4437

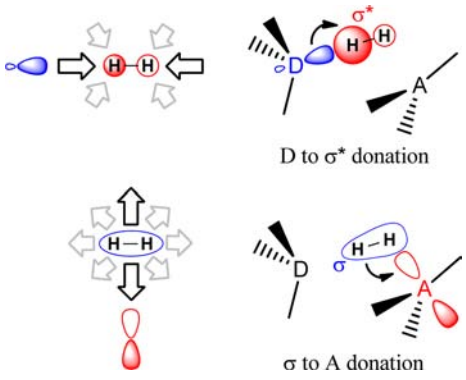

Figure 7. Optimum orientations of interacting orbitals, explaining the bent geometry of the hydrogen splitting TS by FLPs.

end-on−side-on geometry allows an optimal overlap of the frontier orbitals, namely the overlap between the donor sp^2/sp^3-type lone-pair orbital and $\sigma^*(H_2)$, and simultaneously the overlap between the empty p-type orbital of the acceptor with $\sigma(H_2)$.[84,85] The actually observed geometry somewhat deviates from this idealized situation due to the polarization of σ/σ^* leading to optimum $\sigma(H_2)\rightarrow$A overlap at somewhat larger HHA angles (Figure 7, right). Steric constraints arising from the bulky substituents or from the linker also contribute to the deviation from the ideal μ-(η^1,η^2) arrangement. Notably, not only is this approach valid for FLPs, but the geometry of all TSs of hydrogen activation by other systems shown in Figure 1 can also be interpreted by seeking the optimum donor−acceptor overlaps.

Along the H_2 Splitting Pathway. Transition states bear special importance in determining reactivity; nevertheless, further insight can be obtained from monitoring the full pathway on the potential energy surface that connects the reactants and products. Such a study could be beneficial for the H_2 cleavage reaction in particular because the TSs are often quite early, and one of the discussed conceptual models contains explicit references to processes taking place *after* the TS. We therefore analyzed various properties along the IRC,[86] i.e., the minimum energy pathway in mass-weighted internal coordinates, of the H_2 splitting by FLPs. The most relevant results are presented in Figure 8.

Starting from the reactant side, the computed energy profiles (upper graphs in Figure 8) generally begin with a long and flat section with slowly increasing energy, which culminates in the TS, just slightly above the reactants. In this section, H_2 approaches the active centers, and the FLP components get somewhat closer to each other.[87] This part of the energy profile obtained for the reaction with FLP **6** is more "standard" (i.e., the initial section is steeper, leading to a more symmetrical overall profile). The reactant state asymptote of the H−H bond order profiles (middle graphs) is usually 1.0, except for FLPs **3** and **4**. In these cases, the TS is connected to a very shallow local minimum corresponding to an FLP−H_2 complex. These complexes are close both in energy and in geometry to the corresponding TSs, i.e., H_2 still interacts with both the donor and acceptor centers in a μ-(η^1,η^2) fashion with remarkably low D···H and H···A distances.[88] Regardless of the presence of such complexes, the H−H bond orders decrease gradually when approaching the TS region, and as noted before, they reflect a notable degree of H−H bond weakening in the initial phase of the reaction. Somewhat after the TS, an IRC range with a significant and quick decrease of energy (the "drop range") can be observed. This energy change correlates with the sudden decrease of the H−H bond order indicating that this section of the reaction pathway corresponds to the actual bond reorganization process.[89] Along the final, less steep part of the energy profiles, the structural relaxation of the product can be identified, where the H−H bond order eventually decreases to approximately zero.

Concerning the EF, we found that the inhomogeneity illustrated in Figure 5 prevails along the whole reaction pathway. To simplify the presentation, we only show the value of the parallel EF component at the positions of the two H nuclei (lower graphs in Figure 8). As apparent from the graphs, the EF at the H atom closer to the acceptor center (H_A) always increases along the reaction pathway. At least at this nucleus, the field eventually reaches the values necessary for barrierless cleavage (~0.10 au[25]) at some point of the pathway (with the exception of FLP **6**), but our results show that no H_2 *molecule* exists any more in this phase of the reaction.[90] As indicated in Figure 8, at the point where the field strength at H_A increases to 0.1 au, the H−H bond order is typically well below 0.5, and the drop range with the corresponding rapid energy and geometry changes is already in progress for most of the systems.[91] Hence, the bond breakage of H_2 cannot be considered as the result of merely a strong EF. Moreover, if we consider the EF at the other H atom (H_D), we find that its rise becomes gradually less steep than that for H_A, ultimately turning into decrease and leading even to sign change of the parallel field component along the pathway. Apparently, the whole process cannot be qualitatively described as an H_2 molecule entering a "cavity" with strong, appropriately oriented EFs.

The elements of the ET model, however, are consistent with the observations along the whole IRC pathway. As discussed above, the polarization of H_2 via the mixing of the σ and σ^* orbitals, enhancing interactions with both the donor and acceptor already in the TS, can be taken to the limit, when it results in two separate hydrogen s orbitals, which combine with the donor and acceptor orbitals to form the D−H and H−A σ bonds of the product (see Figure 6 above).[24] This model can thus describe a seamless connection between the reactant and product sides, with continuously decreasing H−H bond order and geometry rearrangements occurring when the D−H and H−A interactions become stronger than the H−H one.

Computations and Chemistry in Strong Electric Fields. The key element of the EF model is that the presence of a strong field facilitates the heterolytic cleavage of H_2. In order to support this statement, Grimme and co-workers presented full CI/aug-cc-pVQZ calculations for a H_2 molecule in homogeneous EF and concluded that the splitting barrier essentially disappears at an EF strength of ~0.10 au.[25] They later showed that several DFT functionals with the same basis set also provide comparable results.[26] Nevertheless, these calculations do not take into account one aspect with rather far-reaching consequences. Namely, in an arbitrarily small, but nonzero, homogeneous EF, the bound electronic states of any neutral molecule are metastable with respect to ionization.[93] For weak fields, one can safely neglect this in calculations, but in stronger fields, standard variational quantum chemical calculations like self-consistent field (SCF) and configuration interaction (CI) with large, diffuse basis sets provide a ground-state wave function that describes a partially unbound electronic state.[94,95] Therefore, the resulting electronic energy will be lower than that of the actual bound ground state of the molecule; the more so with increasing basis set size. Full CI

dx.doi.org/10.1021/ja312387q | J. Am. Chem. Soc. 2013, 135, 4425−4437

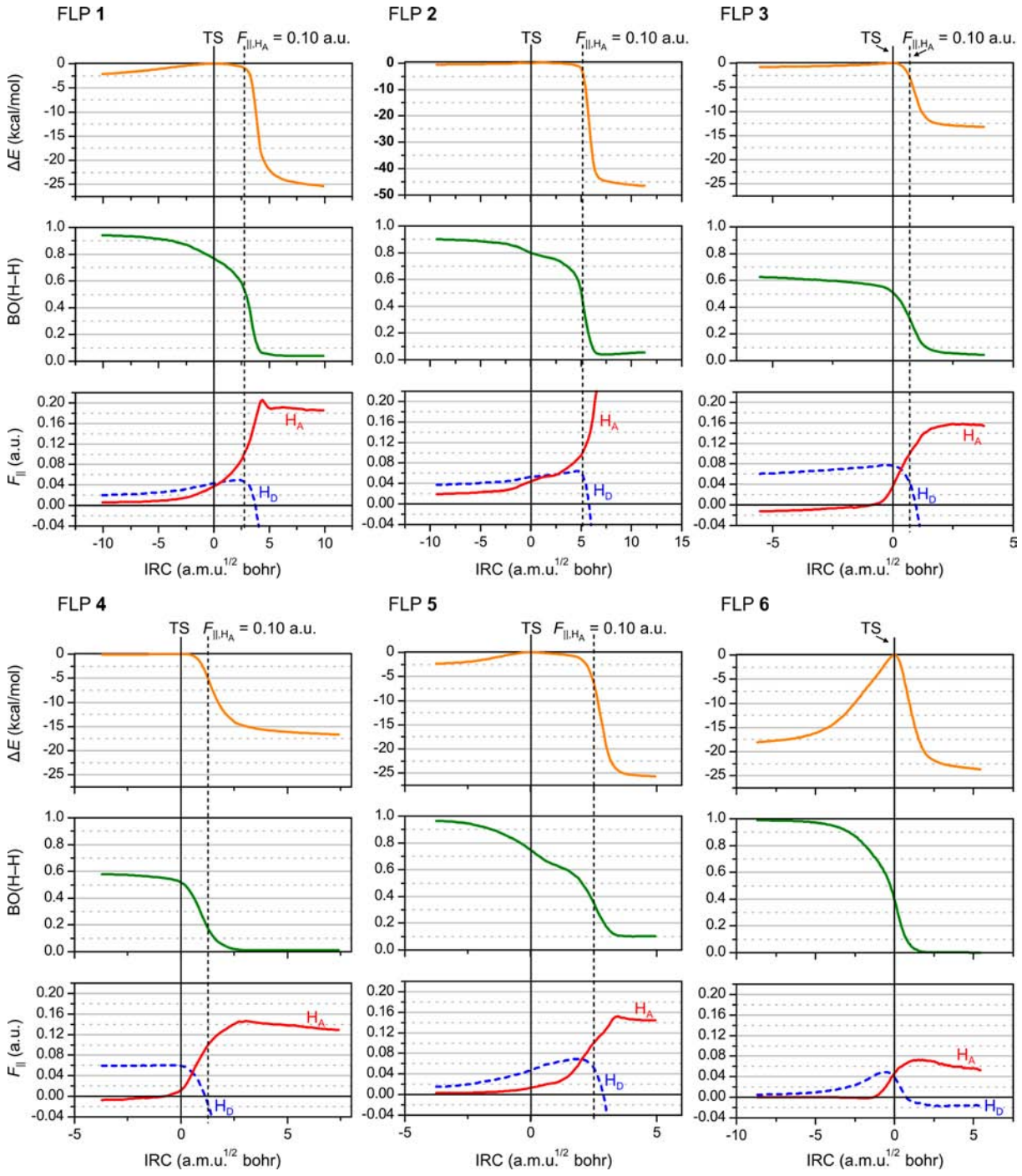

Figure 8. Energies relative to the transition state (ΔE),[92] H–H Mayer bond orders (BO), and the electric field component parallel to the H–H axis ($F_\|$) measured at the positions of the two H nuclei (denoted by H_D and H_A; H_A is closer to the acceptor center), along the intrinsic reaction coordinate pathway for the hydrogen splitting reaction with FLPs **1**–**6**. All data are computed at the ωB97X-D/6-311G(d,p) level. The H atoms of the cleaved H_2 were omitted in the EF calculations. The IRC value is negative in the reactant (FLP + H_2) region and positive in the product (salt/zwitterion) region. Vertical lines indicate the position of the TS (IRC = 0; solid line) and the position where $F_\|$ on the H atom on the acceptor side equals 0.10 au (dashed line). Positive values of $F_\|$ correspond to the direction of the parallel component that facilitates the cleavage.

calculations, while almost exact for H_2 without field with the aug-cc-pVQZ basis, show an extremely large, unphysical basis set dependence for the potential energy surface at a field strength of 0.06–0.10 au.[96]

Fortunately, as metastable electronic states are encountered in various contexts, specialized computational methods providing reasonable results do exist.[97] In his works,[95,98] Saenz has treated the H_2 molecule in strong EFs using the complex scaling method[97] and showed that the barrier for H_2 cleavage still exceeds 20 kcal/mol at 0.10 au, and it is nonzero even at 0.12 au. Hence, our conclusions about the H_2 molecule being cleaved before reaching regions with sufficient EFs for barrierless fission remain valid by an even wider margin. More importantly, the ionization that cannot be treated adequately with common SCF or CI calculations is an actual, physical process, the rate of which can be determined. According to

dx.doi.org/10.1021/ja312387q | J. Am. Chem. Soc. 2013, 135, 4425–4437

Saenz's computations for H_2 at equilibrium H−H distance at a field strength of 0.08 au, the ionization rate exceeds 10^{13} s^{-1}.[95] In an EF where H_2 would split in a (nearly) barrierless process, ionization is thus many orders of magnitude faster than the observed rate of H_2 cleavage with FLPs ($\sim 10^{-5}$–10^{-1} s^{-1}), and it is expected to occur long before the molecule can reach large H−H distances.[98] Qualitatively, H_2 in a strong field would thus undergo ionization, not cleavage. We therefore see no possibility to reconcile in a conceptual model the typical effects of an EF on H_2 with the chemistry occurring in or after the TS of the FLP-mediated H_2 cleavage.

CONCLUSIONS

The electric-field-based reactivity model,[25] consisting of an entrance step providing the barrier and a barrierless cleavage due to a strong electric field, is often considered as the state-of-the-art conceptual description of the frustrated Lewis pair-mediated hydrogen cleavage, superseding the previously published framework suggesting synergistic donor→$\sigma^*(H_2)$ and $\sigma(H_2)$→acceptor electron donations as key elements.[22] Via a computational treatment of six FLPs presented in this work, we contrasted the predictions from both models to see which one is better suited for understanding the essence of the hydrogen activation chemistry. From our analysis, the following conclusions emerged:

1. In the transition state, the H_2 molecule is notably activated according to several criteria, like H−H distance, borane pyramidalization, bond order, or atomic charges. Terming the TS as an "entrance" step in the EF model is misleading, in our opinion, because this concept might imply the involvement of an essentially unactivated H_2.
2. FLPs with similar reactivity show remarkably different field characteristics, in contrast to the suggestion of the EF model. Strong EFs are not present in "cavities" of the FLPs, but only in spherical regions around the donor/acceptor atoms. Accordingly, variation of the EF at the hydrogen nuclei along the reaction pathway does not correspond to the qualitative picture of an H_2 molecule entering a high-field-strength cavity.
3. The EF generated by FLPs in the region of the H nuclei, although capable of accounting for some reduction of the H_2 cleavage barrier, is too small to provide a qualitative interpretation for the electronic structure change and the observed barrier in the TS, or the barrierless cleavage after the TS.
4. Even if the picture of molecular H_2 entering a region with strong fields were correct for the FLPs, the dominant process it would undergo in such a situation is ionization, not cleavage.
5. Donor/acceptor interactions of the FLP with H_2 are present in the TSs for all investigated systems, and they can describe the connection between the reactant and product states and thereby also explain the activated nature of H_2 in the TS. The polarization of H_2 can be interpreted as the result of orbital mixing.
6. The characteristic bent DHHA arrangement in the TS, reminiscent of a μ-(η^1,η^2) coordination, can be rationalized by considering the optimum orbital overlaps for the ET. In contrast, the electric-field-based model provides no explanation for this geometry. The H−H axis is not oriented parallel to the EF direction, and it does not seem obvious, nor has it been described in the literature, what other effects could be taken into consideration within the framework of this model.
7. Computational methods with less satisfactory performance, like B3LYP without dispersion correction, provide somewhat inaccurate TS geometries, but still they describe the correct electronic events occurring upon FLP H_2 activation.

It therefore seems that the originally suggested, electron-donation-based picture of hydrogen splitting by FLPs need not be abandoned, and this class of reactions can be explained analogously to processes occurring at transition metals or various metal−ligand and nonmetal systems. While the effects of the EF are nonnegligible in the quantitative terms of an energy decomposition,[99] and all nuclei and electrons ultimately interact via electrostatic forces, the quantum nature of these particles has a profound influence on the qualitative behavior. For this reason, a simple electric-field-based model provides predictions in stark contrast to the actual computed features even for the initial stages of the reaction. Electron transfer via orbital overlaps has long been a very useful and efficient conceptual tool to interpret the transformations of electronic structure, and it can serve as the basis for the understanding, and thereby the improvement or design, of FLP systems as well.

ASSOCIATED CONTENT

Supporting Information

Comparison of results obtained using various exchange-correlation functionals, D−H and H−A distances vs van der Waals radii, imaginary frequencies, direction of the EF vector, donor and acceptor orbitals of the FLPs, NBO analysis of the electron transfer, illustration of polarization in a four-orbital model, cooperativity in energetics, maximum EF and H−H distance along the IRC, reactant-side H_2 complexes, illustration of calculations in strong EFs, total energies and Cartesian coordinates for the considered stationary points, and complete refs 40 and 41. This material is available free of charge via the Internet at http://pubs.acs.org.

AUTHOR INFORMATION

Corresponding Author

papai.imre@ttk.mta.hu

Notes

The authors declare no competing financial interest.

ACKNOWLEDGMENTS

The authors are grateful to Dr. Tibor Soós and Dr. Tamás Rozgonyi for fruitful discussions. Financial support for this work was provided by the Hungarian Scientific Research Fund (OTKA, grants K-81927 and K-101115). T.A.R. was supported by the János Bolyai Research Scholarship of the Hungarian Academy of Sciences.

REFERENCES

(1) Kubas, G. J. *Chem. Rev.* **2007**, *107*, 4152.
(2) Berke, H. *ChemPhysChem* **2010**, *11*, 1837.
(3) Maseras, F.; Lledós, A.; Clot, E.; Eisenstein, O. *Chem. Rev.* **2000**, *100*, 601.
(4) Hydrogen can also be activated under heterogeneous conditions, e.g., by certain transition metals and metal oxides. The involved electronic mechanisms are similar to those discussed here for homogeneous systems. See: (a) Reference 1. (b) Groß, A. *Theoretical Surface Science—A Microscopic Perspective*, 2nd ed.; Springer: Berlin, Heidelberg, 2009. (c) Hammer, B.; Nørskov, J. *Surf. Sci.* **1995**, *343*,

211. (d) Saillard, J.-Y.; Hoffmann, R. *J. Am. Chem. Soc.* **1984**, *106*, 2006.
(5) de Vries, J. G., Elsevier, C. J., Eds. *The Handbook of Homogeneous Hydrogenation*; Wiley-VCH: Weinheim, 2007.
(6) We note that radical hydrogen cleavage by metal centers with unpaired electrons is also a known reaction, but we do not consider it here in more detail. See, for example: Cui, W.; Wayland, B. B. *J. Am. Chem. Soc.* **2004**, *126*, 8266.
(7) Siegbahn, P. E. M.; Tye, J. W.; Hall, M. B. *Chem. Rev.* **2007**, *107*, 4414.
(8) Involvement of a pendant Lewis *acidic* group together with the transition metal in H_2 activation is rare but not unknown. See, for example: (a) Harman, W. H.; Peters, J. C. *J. Am. Chem. Soc.* **2012**, *134*, 5080. (b) Podiyanachari, S. K.; Fröhlich, R.; Daniliuc, C. G.; Petersen, J. L.; Mück-Lichtenfeld, C.; Kehr, G.; Erker, G. *Angew. Chem., Int. Ed.* **2012**, *51*, 8830.
(9) Frey, G. D.; Lavallo, V.; Donnadieu, B.; Schoeller, W. W.; Bertrand, G. *Science* **2007**, *316*, 439.
(10) Protchenko, A. V.; Birjkumar, K. H.; Dange, D.; Schwarz, A. D.; Vidovic, D.; Jones, C.; Kaltsoyannis, N.; Mountford, P.; Aldridge, S. *J. Am. Chem. Soc.* **2012**, *134*, 6500.
(11) Peng, Y.; Guo, J.-D.; Ellis, B. D.; Zhu, Z.; Fettinger, J. C.; Nagase, S.; Power, P. P. *J. Am. Chem. Soc.* **2009**, *131*, 16272.
(12) Peng, Y.; Ellis, B. D.; Wang, X.; Power, P. P. *J. Am. Chem. Soc.* **2008**, *130*, 12268.
(13) Spikes, G. H.; Fettinger, J. C.; Power, P. P. *J. Am. Chem. Soc.* **2005**, *127*, 12232.
(14) Peng, Y.; Brynda, M.; Ellis, B. D.; Fettinger, J. C.; Rivard, E.; Power, P. P. *Chem. Commun.* **2008**, 6042.
(15) Zhao, L.; Huang, F.; Lu, G.; Wang, Z.-X.; Schleyer, P. v. R. *J. Am. Chem. Soc.* **2012**, *134*, 8856.
(16) Welch, G. C.; San Juan, R. R.; Masuda, J. D.; Stephan, D. W. *Science* **2007**, *314*, 1124.
(17) Welch, G. C.; Stephan, D. W. *J. Am. Chem. Soc.* **2007**, *129*, 1880.
(18) For reviews on FLP chemistry, see: (a) Stephan, D. W.; Erker, G. *Angew. Chem., Int. Ed.* **2010**, *49*, 46. (b) Erker, G. *C.R. Chimie* **2011**, *14*, 831. (c) Stephan, D. W.; Greenberg, S.; Graham, T. W.; Chase, P.; Hastie, J. J.; Geier, S. J.; Farrell, J. M.; Brown, C. C.; Heiden, Z. M.; Welch, G. C.; Ullrich, M. *Inorg. Chem.* **2011**, *50*, 12338. (d) Erker, G. *Dalton Trans.* **2011**, *40*, 7475. (e) Stephan, D. W. *Org. Biomol. Chem.* **2012**, *10*, 5740.
(19) For reviews of related topics referring to FLP chemistry, see: (a) Eisenstein, O.; Crabtree, R. H. *New J. Chem.* **2013**, *37*, 21. (b) Staubitz, A.; Robertson, A. P. M.; Sloan, M. E.; Manners, I. *Chem. Rev.* **2010**, *110*, 4023. (c) De Vries, T. S.; Prokofjevs, A.; Vedejs, E. *Chem. Rev.* **2012**, *112*, 4246. (d) Pihko, P. M.; Rahaman, H. In *Enantioselective Organocatalyzed Reactions I: Enantioselective Oxidation, Reduction, Functionalization and Desymmetrization*; Mahrwald, R., Ed.; Springer Netherlands: Dordrecht, 2011; p 185. (e) Piers, W. E.; Marwitz, A. J. V.; Mercier, L. G. *Inorg. Chem.* **2011**, *50*, 12252. (f) Erker, G. *Organometallics* **2011**, *30*, 358. (g) Bouhadir, G.; Amgoune, A.; Bourissou, D. *Adv. Organomet. Chem.* **2010**, *58*, 1. (h) Whited, M. T. *Beilstein J. Org. Chem.* **2012**, *8*, 1554.
(20) For selected recent contributions on H_2 activation or catalytic hydrogenation with FLPs, see: (a) Bender, G.; Kehr, G.; Daniliuc, C. G.; Dao, Q. M.; Ehrlich, S.; Grimme, S.; Erker, G. *Chem. Commun.* **2012**, *48*, 11085. (b) Bertini, F.; Lyaskovskyy, V.; Timmer, B. J. J.; de Kanter, F. J. J.; Lutz, M.; Ehlers, A. W.; Slootweg, J. C.; Lammertsma, K. *J. Am. Chem. Soc.* **2012**, *134*, 201. (c) Caputo, C. B.; Geier, S. J.; Winkelhaus, D.; Mitzel, N. W.; Vukotic, V. N.; Loeb, S. J.; Stephan, D. W. *Dalton Trans.* **2012**, *41*, 2131. (d) Chapman, A. M.; Haddow, M. F.; Wass, D. F. *J. Am. Chem. Soc.* **2011**, *133*, 18463. (e) Chernichenko, K.; Nieger, M.; Leskelä, M.; Repo, T. *Dalton Trans.* **2012**, *41*, 9029. (f) Erős, G.; Nagy, K.; Mehdi, H.; Pápai, I.; Nagy, P.; Király, P.; Tárkányi, G.; Soós, T. *Chem.—Eur. J.* **2012**, *18*, 574. (g) Farrell, J. M.; Hatnean, J. A.; Stephan, D. W. *J. Am. Chem. Soc.* **2012**, *134*, 15728. (h) Ghattas, G.; Chen, D.; Pan, F.; Klankermayer, J. *Dalton Trans.* **2012**, *41*, 9026. (i) Greb, L.; Oña-Burgos, P.; Kubas, A.; Falk, F. C.; Breher, F.; Fink, K.; Paradies, J. *Dalton Trans.* **2012**, *41*, 9056. (j) Greb, L.; Oña-Burgos, P.; Schirmer, B.; Grimme, S.; Stephan, D. W.; Paradies, J. *Angew. Chem., Int. Ed.* **2012**, *51*, 10164. (k) Herrington, T. J.; Thom, A. J. W.; White, A. J. P.; Ashley, A. E. *Dalton Trans.* **2012**, *41*, 9019. (l) Jiang, C.; Blacque, O.; Fox, T.; Berke, H. *Organometallics* **2011**, *30*, 2117. (m) Kronig, S.; Theuergarten, E.; Holschumacher, D.; Bannenberg, T.; Daniliuc, C. G.; Jones, P. G.; Tamm, M. *Inorg. Chem.* **2011**, *50*, 7344. (n) Lindqvist, M.; Sarnela, N.; Sumerin, V.; Chernichenko, K.; Leskelä, M.; Repo, T. *Dalton Trans.* **2012**, *41*, 4310. (o) Lu, Z.; Cheng, Z.; Chen, Z.; Weng, L.; Li, Z. H.; Wang, H. *Angew. Chem., Int. Ed.* **2011**, *50*, 12227. (p) Mahdi, T.; Heiden, Z. M.; Grimme, S.; Stephan, D. W. *J. Am. Chem. Soc.* **2012**, *134*, 4088. (q) Marwitz, A. J. V.; Dutton, J. L.; Mercier, L. G.; Piers, W. E. *J. Am. Chem. Soc.* **2011**, *133*, 10026. (r) Ménard, G.; Stephan, D. W. *Angew. Chem., Int. Ed.* **2012**, *51*, 8272. (s) Reddy, J. S.; Xu, B.-H.; Mahdi, T.; Fröhlich, R.; Kehr, G.; Stephan, D. W.; Erker, G. *Organometallics* **2012**, *31*, 5638. (t) Schäfer, A.; Reissmann, M.; Schäfer, A.; Saak, W.; Haase, D.; Müller, T. *Angew. Chem., Int. Ed.* **2011**, *50*, 12636. (u) Travis, A. L.; Binding, S. C.; Zaher, H.; Arnold, T. A. Q.; Buffet, J.-C.; O'Hare, D. *Dalton Trans.* **2013**, *42*, 2431. (v) Schulz, F.; Sumerin, V.; Heikkinen, S.; Pedersen, B.; Wang, C.; Atsumi, M.; Leskelä, M.; Repo, T.; Pyykkö, P.; Petry, W.; Rieger, B. *J. Am. Chem. Soc.* **2011**, *133*, 20245.
(21) Welch, G. C.; Cabrera, L.; Chase, P. A.; Hollink, E.; Masuda, J. D.; Wei, P.; Stephan, D. W. *Dalton Trans.* **2007**, 3407.
(22) Rokob, T. A.; Hamza, A.; Stirling, A.; Soós, T.; Pápai, I. *Angew. Chem., Int. Ed.* **2008**, *47*, 2435.
(23) Bakó, I.; Stirling, A.; Bálint, S.; Pápai, I. *Dalton Trans.* **2012**, *41*, 9023.
(24) Hamza, A.; Stirling, A.; Rokob, T. A.; Pápai, I. *Int. J. Quantum Chem.* **2009**, *109*, 2416.
(25) Grimme, S.; Kruse, H.; Goerigk, L.; Erker, G. *Angew. Chem., Int. Ed.* **2010**, *49*, 1402.
(26) Schirmer, B.; Grimme, S. *Chem. Commun.* **2010**, *46*, 7942.
(27) Wiegand, T.; Eckert, H.; Ekkert, O.; Fröhlich, R.; Kehr, G.; Erker, G.; Grimme, S. *J. Am. Chem. Soc.* **2012**, *134*, 4236.
(28) Camaioni, D. M.; Ginovska-Pangovska, B.; Schenter, G. K.; Kathmann, S. M.; Autrey, T. *J. Phys. Chem. A* **2012**, *116*, 7228.
(29) (a) Chai, J.-D.; Head-Gordon, M. *Phys. Chem. Chem. Phys.* **2008**, *10*, 6615. (b) Chai, J.-D.; Head-Gordon, M. *J. Chem. Phys.* **2008**, *128*, 084106. (c) Grimme, S. *J. Comput. Chem.* **2006**, *27*, 1787.
(30) For the 6-311G(d,p) and 6-311++G(3df,3pd) basis sets, see: (a) Krishnan, R.; Binkley, J. S.; Seeger, R.; Pople, J. A. *J. Chem. Phys.* **1980**, *72*, 650. (b) McLean, A. D.; Chandler, G. S. *J. Chem. Phys.* **1980**, *72*, 5639. (c) Clark, T.; Chandrasekhar, J.; Spitznagel, G. W.; Schleyer, P. v. R. *J. Comput. Chem.* **1983**, *4*, 294. (d) Frisch, M. J.; Pople, J. A.; Binkley, J. S. *J. Chem. Phys.* **1984**, *80*, 3265.
(31) Goerigk, L.; Grimme, S. *Phys. Chem. Chem. Phys.* **2011**, *13*, 6670.
(32) Xu, X.; Alecu, I. M.; Truhlar, D. G. *J. Chem. Theory Comput.* **2011**, *7*, 1667.
(33) Zhao, Y.; Truhlar, D. G. *J. Chem. Theory Comput.* **2011**, *7*, 669.
(34) Yang, K.; Zheng, J.; Zhao, Y.; Truhlar, D. G. *J. Chem. Phys.* **2010**, *132*, 164117.
(35) Zhao, Y.; Truhlar, D. G. *Theor. Chem. Acc.* **2008**, *120*, 215.
(36) Zhao, Y.; Truhlar, D. G. *J. Phys. Chem. A* **2005**, *109*, 5656.
(37) Grimme, S.; Antony, J.; Ehrlich, S.; Krieg, H. *J. Chem. Phys.* **2010**, *132*, 154104.
(38) (a) Vosko, S. H.; Wilk, L.; Nusair, M. *Can. J. Phys.* **1980**, *58*, 1200. (b) Lee, C.; Yang, W.; Parr, R. G. *Phys. Rev. B* **1988**, *37*, 785. (c) Becke, A. D. *Phys. Rev. A* **1988**, *38*, 3098. (d) Becke, A. D. *J. Chem. Phys.* **1993**, *98*, 5648. (e) Stephens, P. J.; Devlin, F. J.; Chabalowski, C. F.; Frisch, M. J. *J. Phys. Chem.* **1994**, *98*, 11623.
(39) (a) Hratchian, H. P.; Schlegel, H. B. *J. Chem. Phys.* **2004**, *120*, 9918. (b) Hratchian, H. P.; Schlegel, H. B. *J. Chem. Theory Comput.* **2005**, *1*, 61.
(40) Frisch, M. J.; et al. *Gaussian 09*, Revision A.02; Gaussian, Inc., Wallingford, CT, 2009.
(41) Ahlrichs, R.; et al. *TURBOMOLE 6.3*; University of Karlsruhe, Forschungszentrum Karlsruhe GmbH, TURBOMOLE GmbH, 2011.

(42) (a) Glendening, E. D.; Landis, C. R.; Weinhold, F. *WIREs Comput. Mol. Sci.* **2012**, *2*, 1. (b) Reed, A. E.; Curtiss, L. A.; Weinhold, F. *Chem. Rev.* **1988**, *88*, 899.
(43) Mayer, I. *Chem. Phys. Lett.* **1983**, *97*, 270.
(44) Mayer, I. *BO-SPIN*, Version 1.01; Chemical Research Center, Hungarian Academy of Sciences: Budapest, 2008.
(45) de Marothy, S. *XYZ Viewer 0.97*; Stockholm University, 2010; http://www.physto.se/~sven.
(46) Guo, Y.; Li, S. *Eur. J. Inorg. Chem.* **2008**, 2501.
(47) Stirling, A.; Hamza, A.; Rokob, T. A.; Pápai, I. *Chem. Commun.* **2008**, 3148.
(48) Gao, S.; Wu, W.; Mo, Y. *J. Phys. Chem. A* **2009**, *113*, 8108.
(49) Kim, H. W.; Rhee, Y. M. *Chem.—Eur. J.* **2009**, *15*, 13348.
(50) Li, H.; Zhao, L.; Lu, G.; Mo, Y.; Wang, Z.-X. *Phys. Chem. Chem. Phys.* **2010**, *12*, 5268.
(51) Chase, P. A.; Stephan, D. W. *Angew. Chem., Int. Ed.* **2008**, *47*, 7433.
(52) Holschumacher, D.; Bannenberg, T.; Hrib, C. G.; Jones, P. G.; Tamm, M. *Angew. Chem., Int. Ed.* **2008**, *47*, 7428.
(53) Spies, P.; Erker, G.; Kehr, G.; Bergander, K.; Fröhlich, R.; Grimme, S.; Stephan, D. W. *Chem. Commun.* **2007**, 5072.
(54) Sumerin, V.; Schulz, F.; Atsumi, M.; Wang, C.; Nieger, M.; Leskelä, M.; Repo, T.; Pyykkö, P.; Rieger, B. *J. Am. Chem. Soc.* **2008**, *130*, 14117.
(55) Gao, S.; Wu, W.; Mo, Y. *Int. J. Quantum Chem.* **2011**, *111*, 3761.
(56) Guo, Y.; He, X.; Li, Z.; Zou, Z. *Inorg. Chem.* **2010**, *49*, 3419.
(57) See Table S2 in section S.2 of the SI.
(58) Könczöl, L.; Makkos, E.; Bourissou, D.; Szieberth, D. *Angew. Chem., Int. Ed.* **2012**, *51*, 9521.
(59) (a) Nyhlén, J.; Privalov, T. *Eur. J. Inorg. Chem.* **2009**, 2759. (b) Privalov, T. *Chem.—Eur. J.* **2009**, *15*, 1825.
(60) This feature of H_2 activation/elimination transition states was known before the advent of FLP chemistry. For examples involving main-group compounds, see: (a) Filippov, O. A.; Filin, A. M.; Tsupreva, V. N.; Belkova, N. V.; Lledós, A.; Ujaque, G.; Epstein, L. M.; Shubina, E. S. *Inorg. Chem.* **2006**, *45*, 3086. (b) Scott, A. P.; Golding, B. T.; Radom, L. *New J. Chem.* **1998**, 1171. (c) Chan, B.; Radom, L. *J. Am. Chem. Soc.* **2005**, *127*, 2443.
(61) The transition states for hydrogen splitting by the intermolecular donor/acceptor pairs, particularly **TS$_1$** and **TS$_2$**, are rather flexible even along the imaginary mode due to the predominance of noncovalent interactions and due to their earliness. The flexibility leads to increased sensitivity of the geometrical parameters to the theoretical level used for the optimization. See Table S1 in section S.1 of the SI for a comparison of geometries obtained from various computational methods.
(62) Gonthier, J. F.; Steinmann, S. N.; Wodrich, M. D.; Corminboeuf, C. *Chem. Soc. Rev.* **2012**, *41*, 4671.
(63) Slightly asynchronous formation of the D−H and H−A bonds with H−A being more developed was observed in several works. See refs 20b,o,p, 25, 28.
(64) For a comparison of electronic structure properties computed by various methods, see Table S1 in section S.1 of the SI.
(65) For electric field strength, 1 au ≈ 5.1 × 10^{11} V/m.
(66) See Figure S2 in section S.3 of the SI for an illustration of the direction of the electric field.
(67) H_2 optimized in a homogeneous parallel field of 0.08 au (0.06 au) has a bond order of 0.71 (0.84) at the ωB97X-D/6-311G(d,p) level of theory.
(68) The electric field is strongly inhomogeneous, and even its angle with respect to the H−H direction varies notably along the axis of H_2. Hence, the average angle only provides a rough overall characterization. See Table S3 and Figure S3 in section S.3 of the SI for detailed angle data.
(69) Camaioni and co-workers observed the same ∼45° angle with NH_3 + BX_3 (see ref 28); it thus seems that the tilting is not associated with the presence of bulky substituents.
(70) In ref 27, Eckert, Erker, Grimme, et al. investigated the electric field gradient tensor at the boron nucleus for the datively bound forms of a series of intramolecular P/B FLPs. On the basis of the finding that the largest principal component of this tensor is not parallel to the P···B axis, it was suggested that a linear PHHB geometry is not essential for hydrogen activation. However, the connection relating this tensor component determined in the *datively bound* structure at the position of the *boron atom* to the cleavage of the *hydrogen molecule* occurring in the *datively unbound, active* form was not further explained, nor was any discussion provided rationalizing the specific spatial arrangement of these four atoms in the TS.
(71) See SI, section S.4, Figures S4−S5.
(72) Geier, S. J.; Gilbert, T. M.; Stephan, D. W. *J. Am. Chem. Soc.* **2008**, *130*, 12632.
(73) Guo, Y.; Li, S. *Inorg. Chem.* **2008**, *47*, 6212.
(74) Nyhlén, J.; Privalov, T. *Dalton Trans.* **2009**, 5780.
(75) Lu, G.; Li, H.; Zhao, L.; Huang, F.; Wang, Z.-X. *Inorg. Chem.* **2010**, *49*, 295.
(76) Zhao, L.; Li, H.; Lu, G.; Wang, Z.-X. *Dalton Trans.* **2010**, *39*, 4038.
(77) Geier, S. J.; Gilbert, T. M.; Stephan, D. W. *Inorg. Chem.* **2011**, *50*, 336.
(78) Yang, L.; Ren, X.; Wang, H.; Zhang, N.; Hong, S. *Res. Chem. Intermed.* **2012**, *38*, 113.
(79) See SI, section S.5.
(80) In the real system, electric field and electron transfer effects both contribute to polarization. The key point here is that ET can provide a qualitative interpretation of the phenomenon without invoking the electric field. For a discussion on polarization induced by various interactions including orbital overlap, see: Fujimoto, H.; Inagaki, S. *J. Am. Chem. Soc.* **1977**, *99*, 7424.
(81) To illustrate that H_2 polarization can occur from orbital overlaps without considering an electric field, we present an analysis on a simple MO model in a Hückel-type scheme in section S.6 of the SI.
(82) Mück-Lichtenfeld, C.; Grimme, S. *Dalton Trans.* **2012**, *41*, 9111.
(83) See SI, section S.7.
(84) For the related, directly linked R_2P−BR'_2 systems, the same arguments have been used to explain the analogous geometry of the TS for hydrogen splitting. See ref 59.
(85) These principles have been employed in the computational design of FLP-type compounds. See: (a) Wang, Z.-X.; Lu, G.; Li, H.; Zhao, L. *Chin. Sci. Bull.* **2010**, *55*, 239. (b) Reference 75.
(86) Fukui, K. *Acc. Chem. Res.* **1981**, *14*, 363.
(87) See Figure S8 in section S.8 of the SI for additional graphs along the IRC, including H−H distance.
(88) See section S.9 of the SI for the geometries. Similar complexes have been observed in calculations for a computationally designed pyrazolboranes and carbene-boranes (ref 75), for a computationally designed diphosphineborane (ref 58), and along the H_2 splitting reaction pathways for the $[2,4,6\text{-}(CF_3)_3C_6H_2]_2BH$ diarylborane and triethylamine FLP (ref 20o), as well as for the $B(C_6F_5)_3$ + *N*-alkylaniline (as C-donor) pair (ref 20p). The existence of reactant-side minima with significantly larger D···H and H···A distances, therefore containing essentially unactivated H_2, has also been noted several times. See: (a) References 20b, 22, 28, and 50. (b) Li, H.; Zhao, L.; Lu, G.; Huang, F.; Wang, Z.-X. *Dalton Trans.* **2010**, *39*, 5519. (c) Pyykkö, P.; Wang, C. *Phys. Chem. Chem. Phys.* **2010**, *12*, 149. (d) Wu, D.; Jia, D.; Liu, L.; Zhang, L.; Guo, J. *J. Phys. Chem. A* **2010**, *114*, 11738.
(89) The variation of the H−H bond distance correlates well with the energy change in the drop range; i.e., this section corresponds to bond reorganization also in terms of geometry. See Figure S8 in section S.8 of the SI.
(90) For some of the FLPs and for some values of the reaction coordinate, the maximum value of the parallel component of the electric field over the H−H line segment is higher than the field at either H_A or H_D (see Figure S8 in section S.8 of the SI). However, our conclusion remains valid even if these maximum values are considered.
(91) For NH_3 + BX_3, the NBO analysis indicates disappearance of the H−H bond already at 0.09 au. See ref 28.

(92) The difference between the reactant side energy and the TS energy as this Figure shows does not exactly match the previously discussed barriers for three reasons: (1) Energies along the IRC were calculated with the 6-311G(d,p) basis, while barriers, with the 6-311++G(3df,3pd) basis. (2) The IRC calculations usually fail to converge to the minimum with very high accuracy, while barriers were computed using fully optimized structures. (3) On the reactant side minimum from the IRC, H_2 is still bound to the FLP, either specifically to the donor and acceptor centers (FLPs **3** and **4**; see text) or in a nonspecific way by dispersion. In contrast, barriers were calculated with reference to the isolated H_2 + fully relaxed frustrated complex.
(93) See, e.g.: Drake, G. W. F., Ed. *Springer Handbook of Atomic, Molecular, and Optical Physics*; Springer: New York, 2006.
(94) Luppi, E.; Head-Gordon, M. *Mol. Phys.* **2012**, *110*, 909.
(95) Saenz, A. *Phys. Rev. A* **2002**, *66*, 063407.
(96) For example, the barrier of ∼20 kcal/mol at 0.09 au with aug-cc-pVQZ basis completely disappears with aug-cc-pV6Z basis. See section S.10 of the SI for a detailed demonstration.
(97) For a general overview of metastable states and their treatment, see: Klaiman, S.; Gilary, I. *Adv. Quantum Chem.* **2012**, *63*, 1.
(98) Saenz, A. *Phys. Rev. A* **2000**, *61*, 051402.
(99) For NH_3 + BX_3, this was analyzed in ref 28.